JACS Au
AN OPEN ACCESS JOURNAL OF THE AMERICAN CHEMICAL SOCIETY

pubs.acs.org/jacsau
Article

Decoding the Molecular Basis of the Specificity of an Anti-sTn Antibody

Cátia O. Soares,[‡‡] Maria Elena Laugieri,[‡‡] Ana Sofia Grosso, Mariangela Natale, Helena Coelho, Sandra Behren, Jin Yu, Hui Cai, Antonio Franconetti, Iker Oyenarte, Maria Magnasco, Ana Gimeno, Nuno Ramos, Wengang Chai, Francisco Corzana, Ulrika Westerlind, Jesús Jiménez-Barbero, Angelina S. Palma, Paula A. Videira,* June Ereño-Orbea,* and Filipa Marcelo*

Cite This: *JACS Au* 2025, 5, 225−236
Read Online

ACCESS | Metrics & More | Article Recommendations | Supporting Information

ABSTRACT: The mucin *O*-glycan sialyl Tn antigen (sTn, Neu5Acα2-6GalNAcα1-*O*-Ser/Thr) is an antigen associated with different types of cancers, often linked with a higher risk of metastasis and poor prognosis. Despite efforts to develop anti-sTn antibodies with high specificity for diagnostics and immunotherapy, challenges in eliciting high-affinity antibodies for glycan structures have limited their effectiveness, leading to low titers and short protection durations. Experimental structural insights into anti-sTn antibody specificity are lacking, hindering their optimization for cancer cell recognition. In this study, we used a comprehensive structural approach, combining X-ray crystallography, NMR spectroscopy, computational methods, glycan/glycopeptide microarrays, and biophysical techniques, to thoroughly investigate the molecular basis of sTn recognition by L2A5, a novel preclinical anti-sTn monoclonal antibody (mAb). Our data unequivocally show that the L2A5 fragment antigen-binding (Fab) specifically binds to core sTn moieties. NMR and X-ray structural data suggest a similar binding mode for the complexes formed by the sTn moiety linked to Ser or Thr and the L2A5 Fab. The sugar moieties are similarly oriented in the paratope of mAb, with the Neu5Ac moiety establishing key interactions with the receptor and the GalNAc moiety providing additional contacts. Furthermore, L2A5 exhibits fine specificity toward cancer-related MUC1 and MUC4 mucin-derived sTn glycopeptides, which might contribute to its selective targeting against tumor cells. This newfound knowledge holds promise for the rational improvement and potential application of this anti-sTn antibody in diagnosis and targeted therapy against sTn expressing cancers such as breast, colorectal, and bladder cancer, improving patient care.

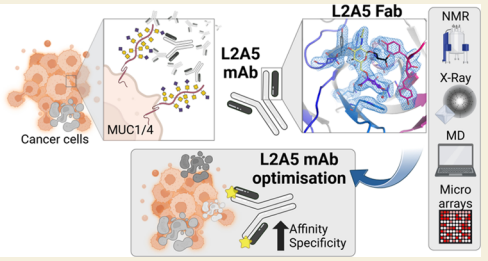

KEYWORDS: *glycan, sialic acid, antibody, NMR, X-ray crystallography*

INTRODUCTION

Abnormal *O*-glycosylation is a hallmark feature in cancer. Different stages of malignancy are characterized by the presence of truncated *O*-glycans, which are often displayed in densely clustered patches of mucin glycoproteins.[1,2] The incomplete synthesis of mucin *O*-glycans results from a deviation from the normal glycosylation pathways in early stages of cancer, yielding shortened chemical structures, truncated mucin *O*-glycans, such as the Tn antigen (GalNAcα1O-Ser/Thr) and the T-antigen (core-1 structure, Galβ1,3GalNAcα1O-Ser/Thr) and their sialylated forms, the sialyl Tn (sTn-, Neu5Acα2-6GalNAcα1O-Ser/Thr) and the sialyl T-antigens (sT-, Neu5Acα2,3Galβ1,3GalNAcα1O-Ser/Thr).[2] In particular, the sTn is overexpressed in diverse types of human epithelial cancers and is associated with higher levels of migration and metastasis, immune suppression, drug resistance, and poor prognosis.[3,4] For that reason, sTn has become an attractive target for developing specific monoclonal antibodies (mAbs) for diagnosis and therapeutic purposes.

Remarkably, the sTn-antigen upregulation mostly occurs due to the overexpression of ST6GalNAc-I throughout a typical disrupted Golgi, instead of normal location at the trans-Golgi cisternae.[5] Thus, ST6GalNAc-I competes with T-synthase (C1GalT1) the enzyme that adds galactose (Gal) to *N*-acetylgalactosamine (GalNAc) to form the core 1, disrupting the canonical glycosylation pathway and precluding further extension of the saccharide chain.[2,5,6] In addition, the lack of active T-synthase (C1GalT1), due to the mutation or silencing of the *Cosmc* chaperone, potentiates the formation of Tn antigen and consequently the generation of the sTn

Received: September 30, 2024
Revised: November 11, 2024
Accepted: November 13, 2024
Published: December 16, 2024

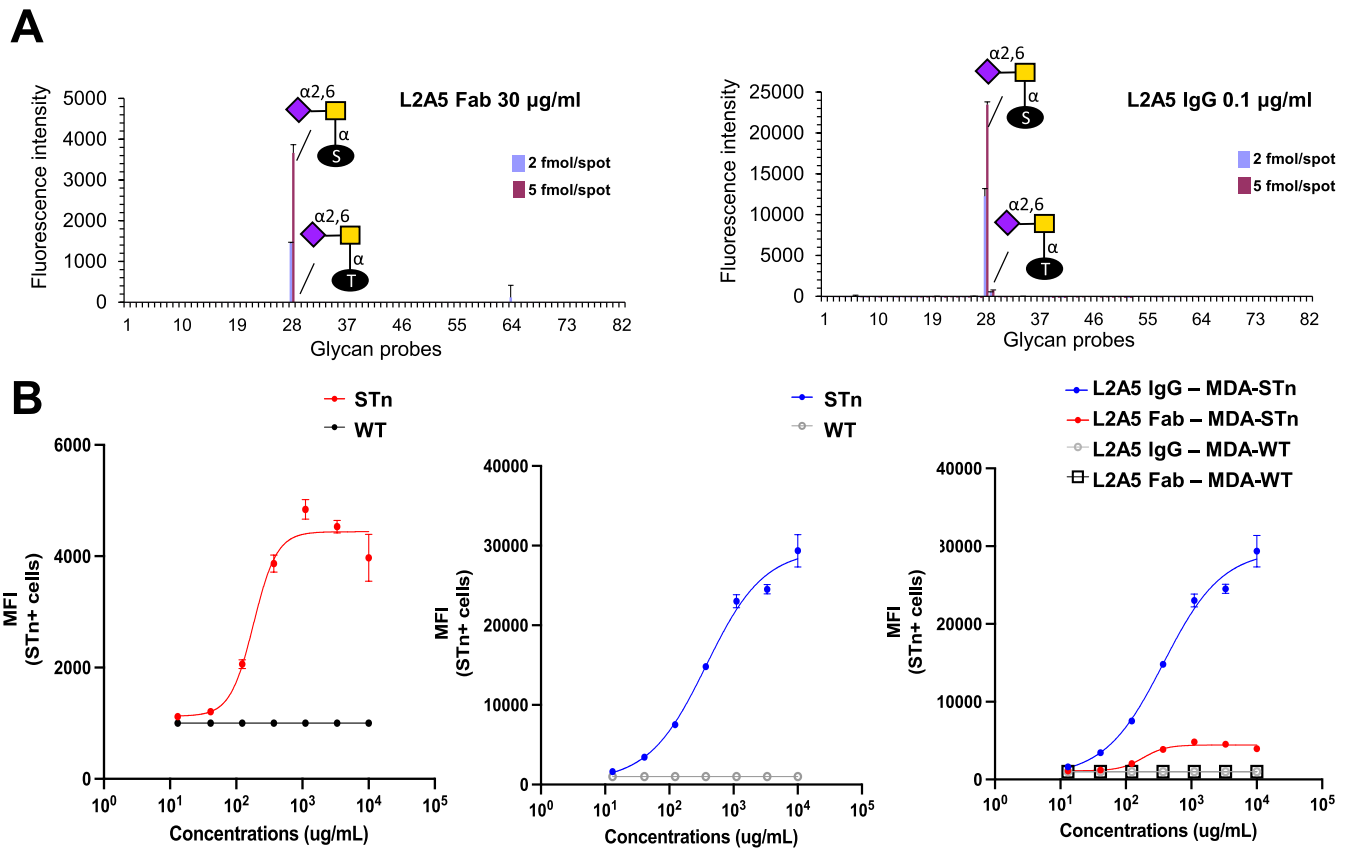

Figure 1. Validation of the L2A5 Fab specificity. (A) Interaction of L2A5 Fab and L2A5 IgG in a focused glycan microarray containing α2−3 and α2−6 sialylated glycans. The full list of probes and their sequences is detailed in Table S1. The chart position assigned to each probe is also referenced in Table S1. (B) Cell binding assays using flow cytometry. Left panel: EC50 MDA-MB231 vs STn expressing cells using L2A5 Fab; Center panel: EC50 MDA-MB231 vs STn expressing cells using L2A5 IgG; Righ panel: EC50 MDA-MB231 vs STn expressing cells using L2A5 Fab vs L2A5 IgG.

through the action of the sialyltransferase ST6GalNAc-I on the Tn.[5−7]

Research efforts have been devoted to developing mAbs that can specifically bind to malignant cells and not to the healthy cells.[8,9] However, currently available antiglycan mAbs typically exhibit rather low affinity and display poor selectivity due to their low immunogenicity and lack of tools to improve their binding features.[3] These characteristics are a limitation for developing efficient antiglycan-based immunotherapies or diagnostic tools suitable for personalized medicine and of interest in the pharma industry. This is especially true for targeting the sTn, since scarce detailed information on the structural basis for its recognition by mAbs has been available so far. Indeed, the access to atomic-resolution information on the molecular recognition features that provide the impetus for the stability of mAb/sTn complexes would be of paramount importance for the development of effective therapeutical mAbs with improved specificity and affinity toward sTn and, eventually, other tumor-associated glycans. However, given the intrinsic flexibility of glycans, such as sTn, there are limited examples of available high-resolution 3D structures of mAb/tumor−glycans complexes,[10−12] none targeting the key sTn. In fact, most of the X-ray crystallography structures of mAb/tumor-glycan complexes have been solved for anti-MUC1 mAbs targeting a specific MUC1 peptide region and not a precise glycan antigen. Most of the structures involved the simple Tn antigen[11,12] and more recently the sT-antigen.[10] In most of those cases, the glycan fragment improves the stability of the MUC1/mAb complex; however, it is not the major driving force for the recognition event (exception 5E5 mAb).[12] Noteworthy, the sTn target offers additional challenges to understanding its recognition, as it exhibits increased flexibility than its precursor Tn, given the presence of the additional sialic acid moiety, which contains additional torsional degrees of freedom.[13,14] Moreover, as all of the reported anti-sTn mAbs depend on sialic acid moieties,[3,15] recognizing Neu5Ac, their poor affinity raises the concern of potential cross-reactivity with other sialoglycans naturally expressed in healthy cells.

Nevertheless, over the years, a variety of anti-sTn mAbs have been developed. Among these, L2A5,[16] B72.3,[17,18] MLS102,[19,20] TKH2,[21,22] HB-STn1,[23] C1282,[24] CC49,[18] 3F1, and those developed by Prendergast et al.[15] are notable. The clinical potential of anti-sTn mAbs is also underscored by Seagen/Pfizer's SGN-STNV antibody-drug conjugate, derived from Prendergast's research, and currently in clinical trials (NCT04665921). Some of these antibodies, including L2A5, B72.3, and Prendergast mAbs have been sequenced. However, despite these advancements, no crystal structures of anti-sTn mAbs have been published, making our upcoming work the first of its kind. Among the described anti-sTn mAbs, the murine L2A5 (IgM isotype) exhibited highly specific binding to short core sTn antigens.[16] Analysis of L2A5 IgM in glycan microarrays with a wide range of sialylated structures demonstrated this fine specificity, showing the ability of the antibody to bind to α2-6-linked sialyl core-1 and α2-6-sialyl

https://doi.org/10.1021/jacsau.4c00921
JACS Au 2025, 5, 225−236

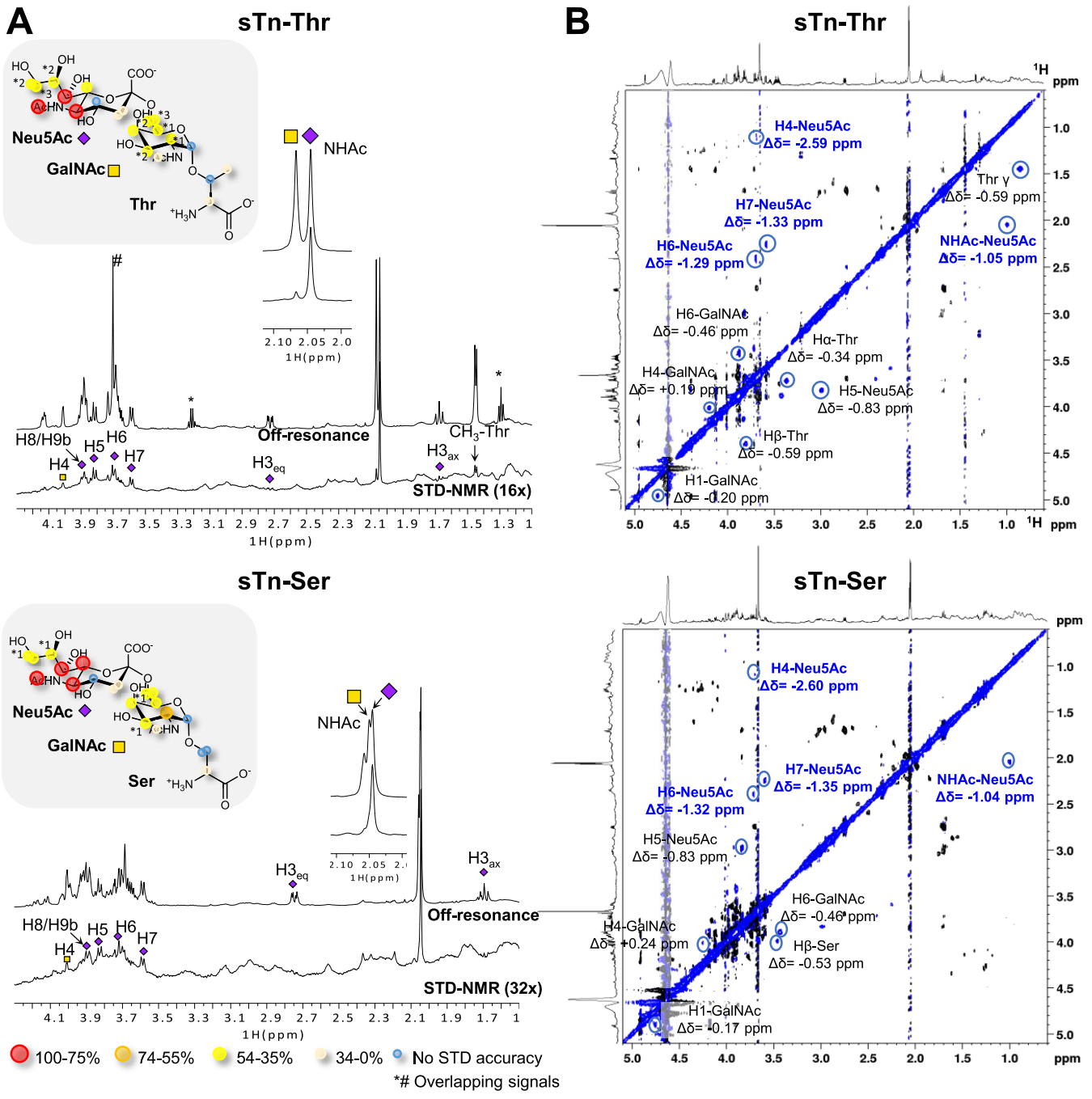

Figure 2. Molecular recognition of sTn−Thr and sTn−Ser by L2A5 Fab. (A) Off-resonance and STD-NMR spectrum of sTn−Thr and sTn−Ser (800 μM) in the presence of L2A5 Fab (20 μM) (40:1 molar ratio) at 310 K and 600 MHz (* ethanol contamination; # Tris). STD-NMR derived epitope map of sTn−Thr and sTn−Ser in the presence of L2A5 Fab is also depicted. The relative STD response is coded according to the legend. (B) TR-ROESY spectrum of sTn−Thr and sTn−Ser (600 μM) in the presence of L2A5 Fab (40 μM) (15:1 molar ratio) at 310 K and 800 MHz. Exchange cross-peaks between the free and bound states are circled and identified with the respective assignment and chemical shift change.

lactose analogue that is present in natural cells, albeit with much weaker affinity, with no binding to other types of sialylated sequences found in glycolipids and glycoproteins of mammalian cells or naturally isolated glycolipids. L2A5 IgM showed binding to sTn-expressing breast, colorectal, and bladder cancer cells, and a distinctive staining pattern of tumor tissue, recognizing regions in invasive and metastasis sites not detectable by other anti-sTn mAbs, and a negligible reactivity to healthy tissues.[16] These features place L2A5 as one of the most sTn-specific mAb reported and an attractive target to be further developed in the clinic.

Since binding affinity does not always directly correlate with pharmacological outcomes, understanding the structural details and kinetics of the binding mode is crucial for optimizing the pharmacological properties of sTn-specific antibodies.[25,26] Therefore, we selected the L2A5 antibody case to develop and implement a structure-based approach for future rational antibody specificity and affinity campaigns. We present the 3D structures of the L2A5 Fab/sTn complexes, using both sTn−

https://doi.org/10.1021/jacsau.4c00921
JACS Au 2025, 5, 225−236

Ser and sTn−Thr antigens as ligands, which have been deduced by using a synergic combination of experimental and computational approaches, including X-ray crystallography, NMR spectroscopy, biophysics, sequence-defined glycan and glycopeptide microarrays, cell binding assays, and molecular dynamics simulations. Our findings demonstrate that the interaction between the L2A5 binding site and sTn is primarily focused on the sialic acid moiety, with additional interactions involving the GalNAc unit contributing to stabilize the complex, underscoring the specificity of the binding mechanism and thus paving the way for antibody's rational design.

RESULTS

L2A5 IgG and Fab Formats Retain Specificity to sTn Antigen

To elucidate the recognition mode of L2A5 mAb and to perform subsequent biophysical and structural analyses, we generated the fragment of the antigen-binding region of L2A5 IgG (L2A5 Fab), which lacks effector function (Figure S1).[27] The specificity for defined glycans of the L2A5 Fab and the L2A5 IgG1 formats, both containing the original mouse antigen-binding variable domains, was first investigated and compared. The glycan binding specificity was assessed using a neoglycolipid (NGL) microarray, which contains structurally distinct glycan sequences displaying both mucin-type *O*-glycan cores (*α*-GalNAc *O*-glycan), *O*-GlcNAc linked to Ser/Thr moieties, *N*-glycans, and lactose and lactosamine-type glycans with diverse decorations, including sialylation (Figure S2, Tables S1 and S2).[28] The analysis in this focused microarray enabled a direct comparison among core *O*-glycan probes that are structurally related to the sialyl-Tn *O*-glycan. The results showed that both antibody formats (Fab and IgG) maintain the predominant binding toward short mucin *O*-glycan core sTn disaccharide NeuAc*α*2−6GalNAc linked to Ser (probe 28) (Figure 1A), as reported for the parental L2A5 IgM analyzed in the same microarray.[16] In line with previous data, cell binding assays using flow cytometry demonstrated that L2A5 Fab and IgG both retain the binding to triple-negative breast cancer cells expressing sTn (MDA-sTn), while they did not bind to the non-sTn expressing parental cells (MDA-WT) (Figure 1B).

As predicted, although the specificity for the sTn is kept, the strength of the interaction with the Fab fragment is weaker than that obtained for the IgG, both detected in glycan microarrays and in the cellular context, which is likely explained by a higher avidity of the bivalent IgG, as also observed for the polyvalent IgM. As reported for the L2A5 IgM, the IgG when tested at a higher concentration of 10 μg/mL, showed the ability to bind to the *α*2−6-sialyl lactose (6′SL) analogue (probe 6) and to the (*α*2−6)-sialyl core-1 (probes 34 and 35), or (*α*2−3, *α*2−6)-disialyl core-1 (probe 36) (Figure S3). In these conditions, the binding to sTn−Ser and sTn−Thr is highly saturated and not accurately quantified. Since the binding of IgG against 6′SL and sialylated core-1 derivatives is overall much weaker than sTn, no binding with the Fab fragment was observed in the glycan microarrays conditions of the analysis. Overall, the high specificity of the Fab and IgG formats of L2A5 to sTn has been confirmed.

Molecular Insights into L2A5 Recognition of Sialoglycans by NMR Spectroscopy

We further analyzed the molecular details of the recognition of the two presentations of the sTn antigen, sTn−Thr and sTn−Ser, by the L2A5 Fab using saturation-transfer-difference (STD) NMR experiments (Figure 2A). STD-NMR provides detailed information on the binding epitope of ligands at the recognition sites of receptors. Interestingly, the STD-derived epitope maps obtained for both sTn−Thr and sTn−Ser (Figure 2A) demonstrated that the Neu5Ac unit is the closest moiety to the L2A5 Fab binding site, with the NHAc group receiving the highest STD response. Weaker STD intensities were observed for the contiguous GalNAc moiety, suggesting a minor involvement of this monosaccharide in the binding event. In agreement, no STD responses were observed in the STD-NMR experiment for Tn−Thr (without sialic acid) in the presence of L2A5 Fab, thus confirming the essential presence of the sialic acid residue for the recognition event (Figure S4).

Additionally, the bound orientation of the antigens in the binding site of the L2A5 Fab was deduced by exchange transferred NOESY experiments (TR-ROESY).[29] Specifically, TR-ROESY experiments for the L2A5 Fab/sTn−Thr and L2A5 Fab/sTn−Ser (Figure 2B) complexes were carried out. In both cases, the NMR spectra showed cross-peaks corresponding to chemical exchange between the free and bound states of the ligands in the L2A5 Fab/sTn complexes. This evidence can be explained by the existence of a free-bound equilibrium that is in the slow exchange regime in the NMR chemical shift time scale, indicating a dissociation constant (K_D) in the low μM range. From a technical NMR perspective, significant upfield chemical shifts were observed for Neu5Ac H4 (−2.59/−2.60 ppm), Neu5Ac H7 (−1.33/−1.35 ppm), Neu5Ac H6 (−1.29/−1.32 ppm), and the *N*-acetyl group of its NHAc moiety (−1.05/−1.04 ppm), strongly supporting that these protons are facing aromatic residues in both sTn-Thr/Ser bound state.

For comparison purposes, the STD-NMR experiment of sTn−Ser in the presence of L2A5 IgG was also accomplished. The STD-derived epitope map of the antigen was very similar to the one described above for the Fab fragment, thus further confirming the resemblance of the specificity and validating that the results obtained for the antigens with the Fab construct are applicable to the IgG L2A5 (Figure S5).

According to previous glycan microarray studies with L2A5 IgM,[16] this antibody weakly cross-reacts with *α*2−6-sialyl lactose (6′SL), but not with *α*2−3-sialyl lactose (3′SL). To assess the specificity of L2A5 with other sialoglycans, we performed STD-NMR experiments for the L2A5 Fab/6'SL mixture and for that with the 3′SL analogue. As expected, under the same experimental conditions for L2A5 Fab/sTn−Thr/Ser complexes, no sizable STD-NMR response was detected for the mixtures with either 3′SL or the Neu5Ac-*α*OMe monosaccharide (Figures S6 and S7). The STD-NMR spectra revealed that L2A5 Fab binds to 6′SL mainly through the Neu5Ac unit (Figure S8A). The corresponding TR-ROESY experiments showed chemical exchange cross-peaks between the free and bound states similar to those described above for the sTn analogues, suggesting a similar binding mode (Figure S8B).

Overall, the NMR spectroscopy, while confirming sTn specificity regardless of its presentation, put in evidence the relevance of the Neu5Ac unit linked in an *α*2−6-sialyl geometry as the proper orientation for L2A5 Fab binding.

https://doi.org/10.1021/jacsau.4c00921
JACS Au 2025, 5, 225−236

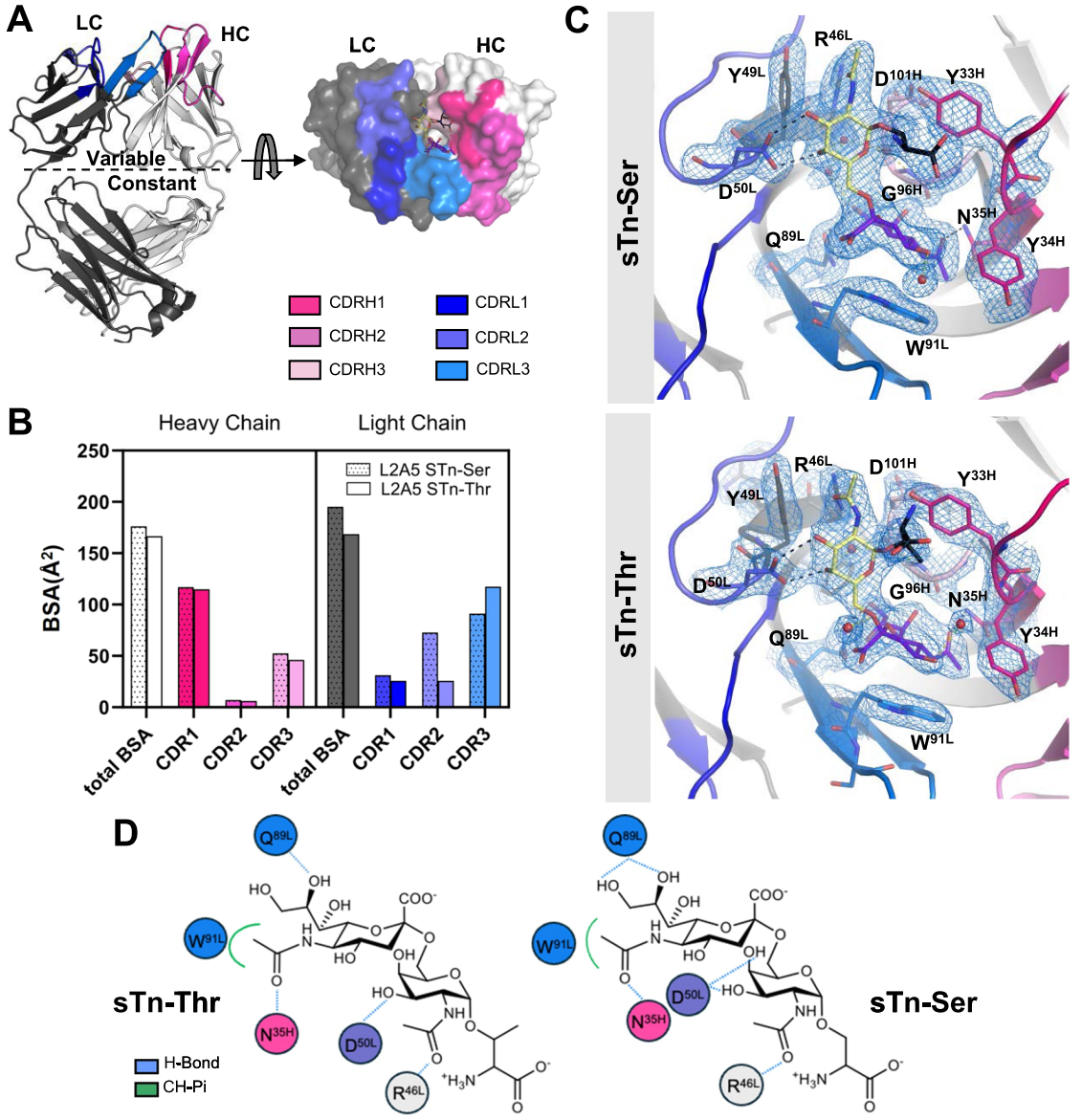

Figure 3. Crystal structure of L2A5 Fab in complex with sTn−Ser or sTn−Thr. (A) Cartoon and surface representation of the side and top views of the crystal structure of the L2A5 Fab. (B) Buried surface area (BSA) values on the L2A5 Fab crystal structures in complex with sTn−Ser or sTn−Thr. (C) Interactions between L2A5 Fab and sTn−Ser and sTn−Thr. H-bonds are depicted with black dashes. Water molecules are shown as red spheres. The composite omit map for sTn−Ser and sTn−Thr, contoured at 1σ, is shown. (D) Schematic representation of the interactions between L2A5 Fab and sTn−Ser and sTn−Thr, respectively.

Molecular Basis of the Interaction between L2A5 and sTn Determined by X-ray Crystallography

Given the challenges posed by glycosylation and the intrinsic flexibility of antibodies in X-ray crystallography, the L2A5 Fab (~50 kDa) was targeted for crystallization studies to elucidate the molecular basis of its recognition mechanism. L2A5 Fab was cocrystallized with the sTn−Ser and sTn−Thr antigens. A variable heavy-chain (V_HH) domain specific for the human kappa light chain (LC) was employed as a well-characterized crystallization chaperone.[30] The crystal structures of L2A5 Fab bound to sTn−Ser and sTn−Thr were successfully obtained at resolutions of 2.3 and 2.6 Å in the *P*212121 and *P*1211 space groups, respectively (Table S3). Two molecules of L2A5 bound to its respective ligand were built in the asymmetric unit (Figure S9).

In the crystal, the bound conformation of sTn−Thr/Ser to L2A5 Fab showed that the α(2,6) Neu5Ac-GalNAc linkage adopts the −g (−60°) and gt (60°) conformers around the φ and ω dihedral angles, respectively (Figure S10). According to NOESY data and molecular modeling, a similar conformational behavior of sTn around φ has been observed when bound to Siglec-15, while around ω, both tg and gt conformers could be adopted.[31] Curiously, the only other X-ray crystal structure of sTn fragment bound to a protein is of a complex with the paired immunoglobulin-like type 2 receptor α (PILRα) (PDB 3WV0), in which the bound conformation is different around the ω dihedral angle, adopting a tg orientation (around 180°).[32]

The analysis of the crystal structures of the L2A5 Fab/sTn−Ser and L2A5 Fab/sTn−Thr complexes revealed a significant contribution of the complementary-determining regions (CDRs) of the LC in comparison to the heavy chain (HC),

https://doi.org/10.1021/jacsau.4c00921
JACS Au 2025, 5, 225−236

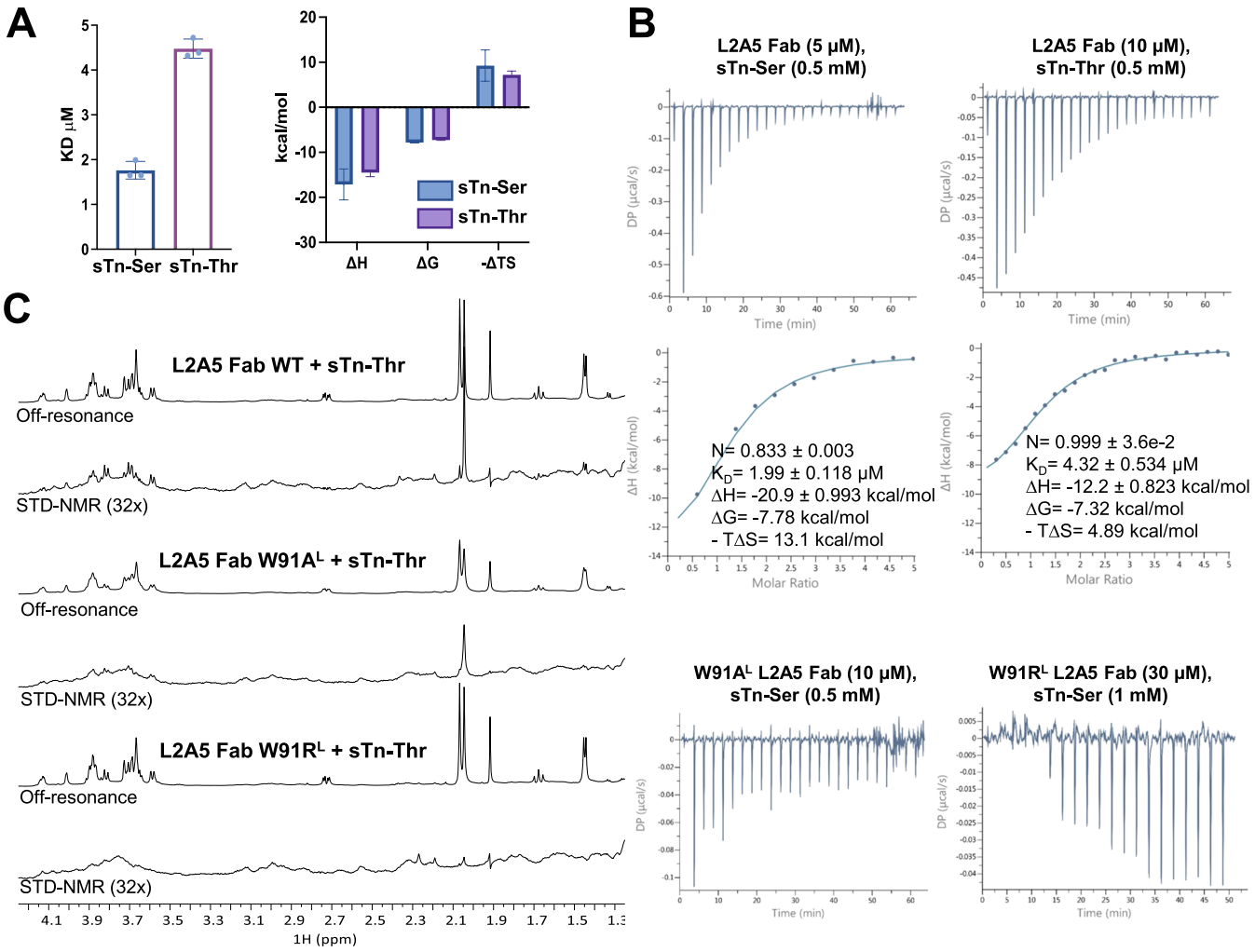

Figure 4. Evaluation of binding of L2A5 Fab WT and W91^{L} mutants to sTn−Thr and sTn−Ser by ITC and NMR. (A) Dissociation constant and thermodynamic parameters obtained from binding of sTn−Ser or sTn−Thr with L2A5 Fab. (B) Representative ITC binding isotherms for binding to sTn−Thr of L2A5 WT, W91A^{L}, and W91R^{L}. (C) Off-resonance and STD-NMR spectra of sTn−Thr (800 μM) in the presence of L2A5 Fab WT, W91A^{L}, and W91R^{L}.

as evidenced by a total buried surface area (BSA) of 171.6 and 166.5 Å^2, respectively (Figure 3). The L2A5 Fab recognizes the Neu5Ac moiety, in agreement with the STD-NMR-derived epitope map described above, highlighting its role in the binding mechanism. The GalNAc moiety establishes less contact with the Fab, while the attached Ser/Thr amino acid residues are exposed to the solvent and their participation in additional noncovalent contacts is marginal (Figure 3). As frequently found in glycan/protein complexes,[33] CH−π interactions take place between the key Neu5Ac moiety and the W91^{L} residue. Fittingly, H4 Neu5Ac is pointing toward the centroid of W91^{L}, as well as the *N*-acetyl group. This binding mode of Neu5Ac, especially the orientation of H4, H6, H7, and NHAc protons of Neu5Ac, with respect to the W91^{L} side chain of L2A5 Fab is in full agreement with the upfield chemical shifts observed for those protons in the bound state in the TR-ROESY NMR spectra (Figure 2B).

From the molecular recognition perspective, multiple intermolecular hydrogen bonds are present that contribute to the recognition of both ligands. Q89^{L} interacts with both Neu5Ac OH8 and OH9, while N35^{H} interacts with the carbonyl group of the Neu5Ac moiety. The intermolecular contacts for GalNAc are essentially the same for both Ser and Thr complexes. D50^{L} participates with a dual donor/acceptor behavior with GalNAc OH-3 and OH-4. In addition, R46^{L} also shows hydrogen bond contact with the *N*-acetyl amide group of the GalNAc moiety.

Having the crystal structure of L2A5 Fab we also assessed by MD simulations the binding poses of 6′SL and 3′SL analogues (Figure S11).

Throughout the simulation, only the complex L2A5 Fab/6′SL was shown to be stable (Figure S11B) and the conformational behavior of 6′SL around the α2,6 linkage was constant (φ = −60°, ψ = 180°, and ω = 60°) (Figure S11C). Four prevalent H-bonds maintain 6′SL in the binding site: D50^{L} establishes H-bonds with OH-3 and OH-4 of Gal, and Q89^{L} and R46^{L} make H-bonds with OH-9 of Neu5Ac (Figure S11D,E). Moreover, CH−π interactions can occur between W91^{L} and H4 and the NHAc group of Neu5Ac (Figure S11D,E). In contrast, the MD simulation of L2A5 Fab with 3′SL revealed that the complex was not stable (Figure S11F). As reflected from these calculations, and in line with NMR data (Figures S6 vs S8), the α2−6-sialyl geometry is essential for the L2A5 recognition event, which is favored by the presence of a contiguous GalNAc/Gal moiety.

https://doi.org/10.1021/jacsau.4c00921
JACS Au 2025, 5, 225−236

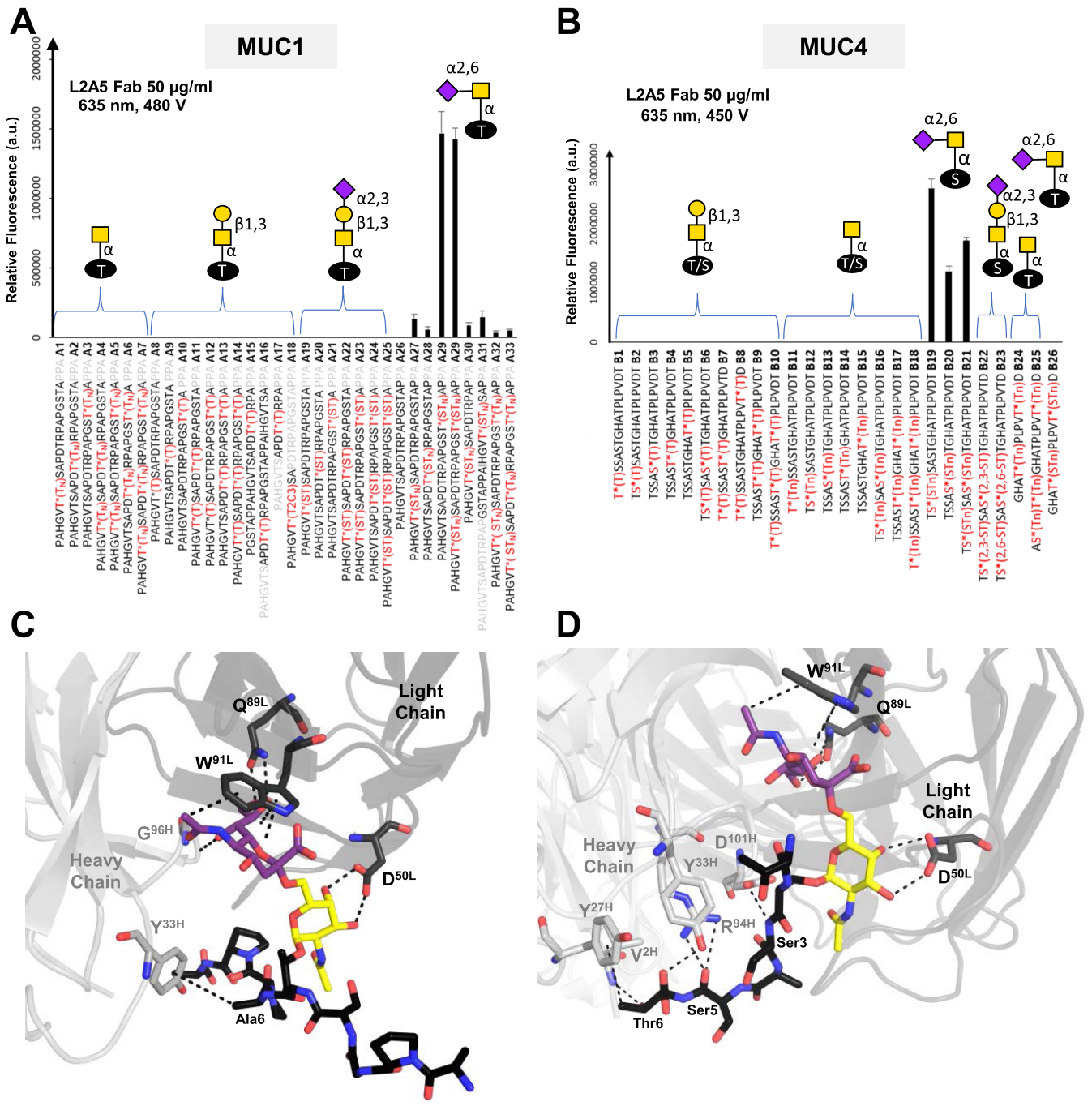

Figure 5. Binding of L2A5 to MUC1 and MUC4 derived glycopeptides. (A) Binding of L2A5 Fab to glycopeptide microarrays of MUC1 derived glycopeptides. (B) Binding of L2A5 Fab to glycopeptide microarrays of MUC4 derived glycopeptides. (C) 3D Model of the L2A5 Fab/APGST*APPA (* = sTn) complex obtained through molecular dynamic simulations. (D) 3D Model of the L2A5 Fab/TS*SAST (* = sTn) complex obtained through molecular dynamic simulations. In (C, D), L2A5 Fab is in cartoon representation (VH in light gray and VL in dark gray), with some residues of the binding site identified and represented in sticks. The glycopeptides are represented in sticks (Neu5Ac, purple; Gal, yellow; peptide, black). Polar interactions and CH−π interactions are depicted with black dashed lines.

W91^{L} Plays a Pivotal Role in the Recognition of sTn by L2A5 mAb

The structural information with atomic resolution was complemented with affinity and thermodynamic data obtained by isothermal titration calorimetry (ITC). The analysis of the ITC experiments with L2A5 Fab and sTn−Ser or sTn−Thr showed a 1:1 stoichiometry for the complexes, with dissociation constants (K_D's) of 1.76 and 4.47 μM, respectively (Figure 4A and Table S4), providing quantitative numbers to the NMR observations. The ITC measurements indicate the existence of a similar thermodynamic profile for the recognition of the two antigens, where the largely favorable enthalpic contribution is counterbalanced by an entropy penalty.

The relevance of the W91^{L} residue in ligand binding that has been inferred from the structural data was further evaluated with ITC experiments (Figure 4B). Remarkably, the mutation of W91^{L} to either a smaller (W91A^{L}) or a positively charged

https://doi.org/10.1021/jacsau.4c00921
JACS Au 2025, 5, 225−236

amino acid (W91R^{L}) led to the complete abrogation of binding to the sTn antigens (sTn−Ser and sTn−Thr), underscoring the pivotal relevance of this W residue in the interaction.

From a structural perspective, the interactions of W91A^{L} and W91R^{L} with sTn−Thr were also tested by STD-NMR and compared with those described above for the L2A5 Fab wild type (WT) (Figure 4C). In the presence of the W91A^{L} variant, sTn−Thr exhibited much less STD-NMR response than the WT, further supporting the much lower affinity of this variant than the WT. Moreover, the STD-NMR response was completely abolished when the W91R^{L} variant was employed.

Further analysis of the stability of the complexes and the persistence of the intermolecular contacts (CH-π and H-bonds) described above was obtained through molecular dynamics (MD) simulations of both L2A5 Fab/sTn−Thr and L2A5 Fab/sTn−Ser complexes (Figures S12 and S13). No major differences were found, and in both cases, the simulations propose a clear role of W91^{L} in the recognition of Neu5Ac, in line with the experimental data.

Searching for Specificity: The Interaction of L2A5 with sTn in MUC1 and MUC4 Glycopeptides

The recognition of tumor-associated mucin tandem repeat (TR) glycopeptides containing the sTn antigen by the L2A5 Fab was further elucidated on glycopeptide microarrays. The arrays contained the variable number tandem repeat (VNTR) peptide sequences of two key membrane mucins in cancer,[34,35] MUC1 and MUC4, decorated with different tumor-associated carbohydrate antigens (Tables S5 and S6). As expected, the L2A5 Fab only recognized peptides glycosylated with the sTn antigen, highlighting the specific binding of L2A5 toward the sTn antigen without any recognition of the Tn-, T-, and the sT−antigens (Figure 5). Interestingly, in the glycopeptide array presentation the anti-sTn, L2A5 Fab recognized both MUC1- and MUC4-derived peptide sequences in a glycosylation site-specific manner. For recognition of MUC1, L2A5 Fab showed a preference for the GST*AP site (**A29**) over the alternative PDT*RP (**A28**) or GVT*SA (**A27**) MUC1 glycosylation sites, in which the * indicates the position of glycosylation by sTn (Figure 5A). An identical preference was also observed in the case of the anti-MUC1 5E5 Ab.[12] Curiously, in 5E5 the main interactions between Tn antigen and 5E5 involve the HC, while in the case of L2A5, it is the LC that mainly contributes to stabilizing the antibody/sTn antigen complex. In the case of MUC4 the sTn−Ser containing glycopeptides (**B19**−**B21**) were better recognized than the sTn−Thr glycopeptide (**B26**); however, it cannot be excluded that the preference in this case could be dependent on the sequence of the glycosylation site (Figure 5B). Among the MUC4 sTn−Ser glycopeptides, the glycosylation of TS*SAST (**B19**) seemed to be favored over the TSSAS*T (**B20**) site.

A 3D view of the interaction of the L2A5 Fab and sTn antigen at PAGST*APPA and TS*SAST of MUC1 and MUC4, respectively, was deduced by MD simulations (Figures 5C,D, S14, and S15). Both complexes were revealed to be stable during the MD simulation (Figures S14 and S15B). In the bound state, sTn−PAGST*APPA displayed the "eclipsed" conformation around the GalNAcα-Thr glycosidic linkage (Ψ1 $\approx$ 120°, Figure S14C) with the sTn moiety oriented perpendicularly to the peptide (Figure 5C). This orientation is the major conformation around the GalNAcα-Thr glycosidic linkage in solution[36] and was previously observed in Tn−glycopeptides complexed with anti-MUC1 mAbs.[12,37] In the case of the sTn−TS*SAST glycopeptide, it adopts the staggered conformation around the GalNAcα-Ser glycosidic linkage (Ψ1 $\approx$ 180°, Figure S15C), where the bound sTn moiety is oriented parallel to the peptide (Figure 5D). This conformation is the most populated conformation found in solution for Tn−Ser glycopeptides.[36] Therefore, the simulations suggest that both sTn−Ser/Thr antigens can fit into the binding site of the antibody, expanding the potential for recognition of these entities. This is in sharp contrast to 5E5, which shows a preference for Tn/sTn linked to Thr.[12]

According to MD simulations, the profile of the intermolecular contacts involving sTn moiety in the selected MUC1 and MUC4 sTn glycopeptides is like those described for L2A5 in complex with sTn−Thr/Ser (Figures S14 and S15D) Notably, additional CH−π interactions between amino acids residues of the sTn-peptide backbone and the antibody (e.g., the methyl group of Ala6 at sTn−PAGST*APPA and Y33^{H} (Figure S14E) and Thr6 at sTn−TS*SAST and Y27^{H} (Figure S15E)), could contribute to stabilize the complex and tentatively explain the observed specificity. Glycopeptide arrays and MD data suggest that the unique peptide backbones and amino acid compositions of the cancer-associated MUC1 and MUC4 glycoproteins might modulate the optimal L2A5 Fab binding interaction with the sTn antigen.

DISCUSSION

Anti *O*-glycan mAbs hold promise as biologics for cancer therapeutics and diagnostics. However, antiglycan mAbs often suffer from low affinity, poor selectivity, and mixed specificity. A detailed characterization at the highest possible resolution of the molecular recognition event between mAbs and glycans is essential to designing or reformatting new antibodies with improved properties. Herein, we have described, at the highest molecular resolution, the driving interactions between a mAb and sTn antigen. We have developed a scientific methodology, synergically combining X-ray crystallography, NMR spectroscopy, biophysics, sequence-defined glycan and glycopeptide microarrays, and cellular assays, along with molecular dynamics simulations, to decode the molecular basis and specificity of L2A5, a patented anti-sTn mAb.[27]

Previous studies have elucidated the binding specificities of anti-MUC1 mAbs, revealing that for the Tn−Ser and Tn−Thr glycopeptides the peptide sequence plays the main impetus for antigen recognition. For instance, the SM3[11] and SN131[10] mAbs target mainly the DTR region of MUC1 sequence. However, both antibodies show a stronger affinity for tumor-associated glycopeptides (SM3/Tn−DTR 0.45 μM; SN131/sT-DTR 1.58 nM) over the corresponding naked peptides (SM3/DTR 1.4 μM; SN131/DTR 10.8 μM). Conversely, the 5E5 mAb[12] exhibits high specificity for the GalNAc moiety in the GST*A region of MUC1 peptide sequence, preferring the Tn- (0.96 μM) over sTn antigen (19 μM). Achieving specificity for anti-sTn mAbs is more challenging than that for anti-MUC1 Abs, as they need to target the external Neu5Ac moiety, a component also found in the sialoglycans of healthy cells. This raises concerns about potential cross-reactivity with healthy tissues.

Among the available anti-sTn mAbs, L2A5 has stood out for its reported specificity toward sialylated structures on the cell surface of sTn-expressing cancers, including breast, colorectal, and bladder cancers, and insignificant reactivity to healthy tissues.[16] Glycan microarray analyses have conclusively

https://doi.org/10.1021/jacsau.4c00921
JACS Au 2025, 5, 225−236

demonstrated that L2A5, in both its Fab and IgG formats, specifically binds to mucin core sTn moieties. A weaker affinity for α2−6-sialyl lactose in comparison to sTn antigen was detected for the IgG L2A5 Ab version in the array.

Remarkably, our study provides the molecular basis for the binding specificity of the α2−6-Neu5Ac geometry by L2A5 mAb and key structural insights into this preclinical anti-sTn mAb. NMR and X-ray structural data suggest the existence of a similar binding mode for the complexes formed by sTn−Ser/Thr with the L2A5 Fab. Ser and Thr amino acids are exposed to the solvent, which suggests minimal participation in noncovalent contacts. The sugar moieties are oriented similarly in the mAb binding site with the Neu5Ac moiety establishing the key interactions with the receptor and the GalNAc moiety providing additional contacts and contributing to stabilizing the complex.

The glycopeptide array suggests that L2A5 Fab preferentially binds the sTn−Thr antigen at the GST*AP sequence of MUC1 and sTn−Ser at the TS*SAST of MUC4. This result highlights the importance of the underlying peptide sequence in the fine specificity and binding of L2A5 and pinpoints that the differences in binding to sTn−Ser and sTn−Thr should certainly be further explored in the context of a specific peptide backbone.

However, the MUC1 and MUC4 specific recognition suggested by microarrays likely contributes to the selective targeting of tumor cells over healthy cells beyond the recognition of the sTn antigen alone. Notably, aberrant glycosylation of MUC1 and MUC4 at TR domains are prevalent in various tumors with a strong impact in cancer progression, immune modulation, and metastasis.[34,35] Thus, this selective binding to tumor-associated mucins could be further emphasized as a critical factor in the therapeutic targeting of cancer cells.

When comparing the amino acid sequences of the VL and VH of the L2A5 mAb to those of other four anti-sTn mAbs that have been described to be specific for sTn (TKH2,[22] 3F1, 8C2−2D6, and 2G12−2B2[15]), we can find common structural features (Figure S16). Overall, the last three sequences share certain similarities (despite the existence of a longer sequence for the CDRL1 region of 2G12−2B2), while L2A5 and TKH2 are rather distinct. Structural data for TKH2 have been reported, derived from mutation studies assisted by STD-NMR and computational calculations.[38] For TKH2, the main residues for sTn binding are $W52^H$ and $Q89^L$, which interact with the methyl of NHAc and glycerol portions of Neu5Ac, respectively, and $W91^L$, which establishes a stacking interaction with the GalNAc moiety. Although $W52^H$ is not conserved in L2A5, $Q89^L$, and $W91^L$ are present in both sequences (in the CDRL3). However, while $Q89^L$ in L2A5 and TKH2 interacts with the Neu5Ac glycerol side chain, $W91^L$ in L2A5 interacts with the Neu5Ac moiety and not the contiguous GalNAc unit, as described for TKH2. Although these antibodies share specificity for sTn as well as structural and sequence similarities, the fine details of the recognition modes are different (Figure S17). Key amino acids (Q and W) are present in both cases, but subtle modifications of their relative orientations provide a different recognition mechanism. From this comparison, it is tempting to speculate that achieving proper orientation of two sets of W and Q residues to simultaneously target both the Neu5Ac (as in L2A5) and the GalNAc moieties (as in TKH2) could be the key to further improving the sTn selectivity and to achieve a much better anti-sTn antibody.

Our findings highlight the detailed molecular interactions that underline L2A5′s specificity for the sTn antigen. However, a scarce number of hydrogen bonds are established between the sTn moiety and the L2A5′s binding site (as in the case of TKH2). In addition, the carboxylic acid of the Neu5Ac moiety is not directly engaged in the recognition process. These features can explain the still low affinity deduced for L2A5′s Fab by ITC. In this perspective, precise site point mutations to increase the number of hydrogen bonds and to establish a potential salt-bridge interaction with the carboxylic acid will certainly increase affinity and improve the specificity of L2A5 toward sTn antigen. Finally, the fact that the MUC1 and MUC4 peptide sequence in sTn glycopeptides could modulate L2A5 Ab binding can be used to design additional peptide/antibody contacts that would improve recognition of L2A5 targeting cancer cells, and our structural model provides a platform for respective efforts. A similar concept was recently exploited in the development of new Tn- and sTn antibodies that specifically recognize the Tn-/sTn- and peptide epitopes.[39]

While our findings contribute to enhance selective cancer cell targeting, additional characterization in cellular and tissues contexts is needed to fully validate L2A5′s clinical potential.

CONCLUSIONS

For the first time, high-resolution information on sTn antigen recognition by a mAb is provided. Specifically, the binding mechanism of the preclinical anti-sTn mAb L2A5 to sTn was fully scrutinized. This new knowledge sets the stage for rational chemical engineering of enhanced anti-sTn L2A5 Ab. Specifically, our data show significant potential for better applications of anti-sTn mAbs in diagnosing and treating cancers that express sTn, like breast, colorectal, and bladder cancer. This advancement will ultimately lead to improved patient care.

Although new advances in the application of artificial intelligence methods for protein design are rapidly advancing, achieving selectivity for the recognition of a specific glycan remains elusive. New detailed experimental structures of antiglycan antibodies are thus required to foster these advances. In this perspective, the structural approach herein reported is robust and can be extended to accelerate the humanization process of distinct antiglycan antibodies and to improve their specificities and affinities, strongly contributing to the research field of antibodies.

MATERIALS AND METHODS

A detailed description of the experimental methods and protocols is included in the Supporting Information.

ASSOCIATED CONTENT

Data Availability Statement

All data needed to evaluate the conclusions in the paper are present in the main text and/or the Supporting Information. Crystal structure models have been deposited in the Protein Data Bank under deposition numbers 9FY8 and 9FXT.

Supporting Information

The Supporting Information is available free of charge at https://pubs.acs.org/doi/10.1021/jacsau.4c00921.

https://doi.org/10.1021/jacsau.4c00921
JACS Au 2025, 5, 225−236

Material and methods include all of the experimental details for the construct design, expression and purification of L2A5 Fab, glycan and glycopeptide microarrays, NMR spectroscopy, crystallization, X-ray data collection and structure solution, isothermal titration calorimetry, cell binding assay by flow cytometry, molecular dynamics simulations and synthesis of glycopeptide used in glycopeptide microarrays (Figures S1−S17) (Tables S1−S6) (PDF)

AUTHOR INFORMATION

Corresponding Authors

Paula A. Videira − *UCIBIO—Applied Molecular Biosciences Unit, Department of Chemistry, NOVA School of Science and Technology, NOVA University Lisbon, 2829-516 Caparica, Portugal; Associate Laboratory i4HB, Institute for Health and Bioeconomy, NOVA School of Science and Technology, NOVA University Lisbon, 2829-516 Caparica, Portugal*; Email: p.videira@fct.unl.pt

June Ereño-Orbea − *CIC bioGUNE, Basque Research and Technology Alliance, E-48160 Derio, Spain; Ikerbasque Basque Foundation for Science, 48009 Bilbao, Bizkaia, Spain*; orcid.org/0000-0002-5076-2105; Email: jereno@cicbiogune.es

Filipa Marcelo − *UCIBIO—Applied Molecular Biosciences Unit, Department of Chemistry, NOVA School of Science and Technology, NOVA University Lisbon, 2829-516 Caparica, Portugal; Associate Laboratory i4HB, Institute for Health and Bioeconomy, NOVA School of Science and Technology, NOVA University Lisbon, 2829-516 Caparica, Portugal*; orcid.org/0000-0001-5049-8511; Email: filipa.marcelo@fct.unl.pt

Authors

Cátia O. Soares − *UCIBIO—Applied Molecular Biosciences Unit, Department of Chemistry, NOVA School of Science and Technology, NOVA University Lisbon, 2829-516 Caparica, Portugal; Associate Laboratory i4HB, Institute for Health and Bioeconomy, NOVA School of Science and Technology, NOVA University Lisbon, 2829-516 Caparica, Portugal*

Maria Elena Laugieri − *CIC bioGUNE, Basque Research and Technology Alliance, E-48160 Derio, Spain*

Ana Sofia Grosso − *UCIBIO—Applied Molecular Biosciences Unit, Department of Chemistry, NOVA School of Science and Technology, NOVA University Lisbon, 2829-516 Caparica, Portugal; Associate Laboratory i4HB, Institute for Health and Bioeconomy, NOVA School of Science and Technology, NOVA University Lisbon, 2829-516 Caparica, Portugal*

Mariangela Natale − *UCIBIO—Applied Molecular Biosciences Unit, Department of Chemistry, NOVA School of Science and Technology, NOVA University Lisbon, 2829-516 Caparica, Portugal; Associate Laboratory i4HB, Institute for Health and Bioeconomy, NOVA School of Science and Technology, NOVA University Lisbon, 2829-516 Caparica, Portugal*

Helena Coelho − *UCIBIO—Applied Molecular Biosciences Unit, Department of Chemistry, NOVA School of Science and Technology, NOVA University Lisbon, 2829-516 Caparica, Portugal; Associate Laboratory i4HB, Institute for Health and Bioeconomy, NOVA School of Science and Technology, NOVA University Lisbon, 2829-516 Caparica, Portugal*; orcid.org/0000-0003-1992-8557

Sandra Behren − *Department of Chemistry, Umeå University, 90187 Umeå, Sweden*

Jin Yu − *Department of Chemistry, Umeå University, 90187 Umeå, Sweden; Glycosciences Laboratory, Faculty of Medicine, Imperial College London, London W12 0NN, U.K.*

Hui Cai − *Department of Chemistry, Umeå University, 90187 Umeå, Sweden; School of Pharmaceutical Sciences, Sun Yat-Sen University, Guangzhou, Guangdong 510275, China*; orcid.org/0000-0002-5394-8167

Antonio Franconetti − *CIC bioGUNE, Basque Research and Technology Alliance, E-48160 Derio, Spain*

Iker Oyenarte − *CIC bioGUNE, Basque Research and Technology Alliance, E-48160 Derio, Spain*

Maria Magnasco − *CIC bioGUNE, Basque Research and Technology Alliance, E-48160 Derio, Spain*

Ana Gimeno − *CIC bioGUNE, Basque Research and Technology Alliance, E-48160 Derio, Spain*; orcid.org/0000-0001-9668-2605

Nuno Ramos − *UCIBIO—Applied Molecular Biosciences Unit, Department of Chemistry, NOVA School of Science and Technology, NOVA University Lisbon, 2829-516 Caparica, Portugal; Associate Laboratory i4HB, Institute for Health and Bioeconomy, NOVA School of Science and Technology, NOVA University Lisbon, 2829-516 Caparica, Portugal*

Wengang Chai − *Glycosciences Laboratory, Department of Metabolism, Digestion and Reproduction, Imperial College London, London SW7 2AZ, U.K.*; orcid.org/0000-0003-2977-5347

Francisco Corzana − *Departamento de Química, Instituto de Investigación en Química de la Universidad de La Rioja (IQUR), Universidad de La Rioja, 26006 Logroño, La Rioja, Spain*; orcid.org/0000-0001-5597-8127

Ulrika Westerlind − *Department of Chemistry, Umeå University, 90187 Umeå, Sweden*

Jesús Jiménez-Barbero − *CIC bioGUNE, Basque Research and Technology Alliance, E-48160 Derio, Spain; Ikerbasque Basque Foundation for Science, 48009 Bilbao, Bizkaia, Spain; Department of Organic and Inorganic Chemistry, Faculty of Science and Technology, University of the Basque Country, EHU-UPV, 48940 Leioa, Bizkaia, Spain; Centro de Investigacion Biomedica En Red de Enfermedades Respiratorias, 28029 Madrid, Spain*; orcid.org/0000-0001-5421-8513

Angelina S. Palma − *UCIBIO—Applied Molecular Biosciences Unit, Department of Chemistry, NOVA School of Science and Technology, NOVA University Lisbon, 2829-516 Caparica, Portugal; Associate Laboratory i4HB, Institute for Health and Bioeconomy, NOVA School of Science and Technology, NOVA University Lisbon, 2829-516 Caparica, Portugal*

Complete contact information is available at: https://pubs.acs.org/10.1021/jacsau.4c00921

Author Contributions

‡‡C.O.S. and M.E.L.: co-first authors. Experimental conception and design: J.E.-O., F.M.; data acquisition: C.O.S., M.E.L., A.S.G., M.N., I.O., M.M., S.B., J.Y., H.C, U.W., A.S.P.; analysis of data: C.O.S., H.Co., M.E.L., A.F., A.G., A.S.G., F.C., W.C., N.R., S.B., U.W., J.J.-B., A.S.P., J.E.-O., F.M.; drafting the article or revising it critically for important intellectual content: C.O.S., M.E.L., J.J.-B., A.S.P., P.A.V., J.E.-O., F.M. CRediT: **Cátia Oliveira Soares** formal analysis, investigation, method-

https://doi.org/10.1021/jacsau.4c00921
JACS Au 2025, 5, 225−236

ology, writing - original draft, writing - review & editing; **Maria Elena Laugieri** formal analysis, investigation, methodology, writing - original draft, writing - review & editing; **Ana Sofia Grosso** formal analysis, investigation, methodology; **Mariangela Natale** formal analysis, investigation, methodology; **Helena Nobre Coelho** data curation, formal analysis, methodology; **Sandra Behren** data curation, formal analysis, methodology; **Jin Yu** formal analysis; **Hui Cai** formal analysis; **Antonio Franconetti** formal analysis; **Iker Oyenarte** formal analysis; **Maria Magnasco** formal analysis; **Ana Gimeno** formal analysis; **Nuno Ramos** validation; **Wengang Chai** validation; **Francisco Corzana** methodology, software, supervision, validation, writing - review & editing; **Ulrika Westerlind** data curation, formal analysis, methodology, supervision, validation, writing - review & editing; **Jesús Jiménez-Barbero** funding acquisition, resources, supervision, validation, writing - review & editing; **Angelina Palma** data curation, formal analysis, funding acquisition, methodology, validation, writing - review & editing; **Paula A. Videira** funding acquisition, resources, supervision, validation, writing - review & editing; **June Ereno-Orbea** conceptualization, formal analysis, funding acquisition, investigation, methodology, resources, supervision, validation, writing - original draft, writing - review & editing; **Filipa Marcelo** conceptualization, formal analysis, funding acquisition, investigation, methodology, resources, supervision, validation, writing - original draft, writing - review & editing.

Notes

The authors declare the following competing financial interest(s): N.R. and M.N. were employed by CellmAbs Biopharmaceuticals. N.R. and P.A.V. are co-founders and shareholders of CellmAbs. Additionally, P.A.V., A.S.P., and W.C. are named as inventors on patent WO2019147152.

■ ACKNOWLEDGMENTS

This work is funded by the European Union under Horizon Europe (project 101079417 — GLYCOTwinning). F.M. and H.Co. also acknowledge FCT-Portugal to the CEECINST/00042/2021 and 10.54499/2020.03261.CEECIND/CP1586/CT0012 research contracts, respectively. C.O.S. and A.S.G thank FCT-Portugal for the PhD grant 2022.11723.BD and COVID/BD/152986/2023, respectively. F.M., C.O.S., A.S.G., and H.Co. acknowledge Fundação para a Ciência e a Tecnologia (FCT-Portugal) for the funding UIDP/04378/2020 and UIDB/04378/2020 to UCIBIO research unit and LA/P/0140/2020 to the i4HB Associate Laboratory. P.A.V. also thanks project InnoGlyco (ref: 2022.04607.PTDC). The authors also thank Agencia Estatal de Investigación of Spain (PID2021-127662OB-I00 to F.C. and PID2019-107770RA-I00 to J.E.-O), the Juan de la Cierva Formación 2021 (FJC2021-046465-I to M.E.L). J.J.-B, J.E.-O, and M.E.L. also thank the Severo Ochoa Center of Excellence Accreditation CEX2021-001136-S, all funded by MCIN/AEI/10.13039/501100011033 and by El FSE invierte en tu futuro, as well as CIBERES, and initiative of Instituto de Salud Carlos III (ISCIII, Spain). The NMR spectrometers are part of the National NMR Network (PTNMR) and were partially supported by Infrastructure Project No 22161 (cofinanced by FEDER through COMPETE 2020, POCI and PORL and FCT through PIDDAC). X-ray diffraction experiments described in this paper were performed using beamline i24 at Diamond Light Source (Oxfordshire, UK).

■ REFERENCES

(1) Reily, C.; Stewart, T. J.; Renfrow, M. B.; Novak, J. Glycosylation in health and disease. *Nat. Rev. Nephrol.* **2019**, *15*, 346−366.
(2) Pinho, S. S.; Reis, C. A. Glycosylation in cancer: mechanisms and clinical implications. *Nat. Rev. Cancer* **2015**, *15*, 540−555.
(3) Julien, S.; Videira, P. A.; Delannoy, P. Sialyl-tn in cancer: (how) did we miss the target? *Biomolecules* **2012**, *2*, 435−466.
(4) Julien, S.; Lagadec, C.; Krzewinski-Recchi, M. A.; et al. Stable expression of sialyl-Tn antigen in T47-D cells induces a decrease of cell adhesion and an increase of cell migration. *Breast Cancer Res. Treat.* **2005**, *90*, 77−84.
(5) Sewell, R.; Bäckström, M.; Dalziel, M.; et al. The ST6GalNAc-I Sialyltransferase Localizes throughout the Golgi and Is Responsible for the Synthesis of the Tumor-associated Sialyl-Tn O-Glycan in Human Breast Cancer. *J. Biol. Chem.* **2006**, *281*, 3586−3594.
(6) Pearce, O. M. T. Cancer glycan epitopes: biosynthesis, structure and function. *Glycobiology* **2018**, *28*, 670−696.
(7) Ju, T.; Lanneau, G. S.; Gautam, T.; et al. Human Tumor Antigens Tn and Sialyl Tn Arise from Mutations in Cosmc. *Cancer Res.* **2008**, *68*, 1636−1646.
(8) Haji-Ghassemi, O.; Blackler, R. J.; Young, N. M.; Evans, S. V. Antibody recognition of carbohydrate epitopes†. *Glycobiology* **2015**, *25*, 920−952.
(9) Manimala, J. C.; Roach, T. A.; Li, Z.; Gildersleeve, J. C. High-throughput carbohydrate microarray profiling of 27 antibodies demonstrates widespread specificity problems. *Glycobiology* **2007**, *17*, 17C−23C.
(10) Wakui, H.; Yokoi, Y.; Horidome, C.; et al. Structural and molecular insight into antibody recognition of dynamic neoepitopes in membrane tethered MUC1 of pancreatic cancer cells and secreted exosomes. *RSC Chem. Biol.* **2023**, *4*, 564−572.
(11) Martínez-Sáez, N.; Castro-López, J.; Valero-González, J.; et al. Deciphering the Non-Equivalence of Serine and Threonine O-Glycosylation Points: Implications for Molecular Recognition of the Tn Antigen by an anti-MUC1 Antibody. *Angew. Chem., Int. Ed.* **2015**, *54*, 9834.
(12) Macías-León, J.; Bermejo, I. A.; Asín, A.; et al. Structural characterization of an unprecedented lectin-like antitumoral anti-MUC1 antibody. *Chem. Commun.* **2020**, *56*, 15137−15140.
(13) Soares, C. O.; Grosso, A. S.; Ereño-Orbea, J.; Coelho, H.; Marcelo, F. Molecular Recognition Insights of Sialic Acid Glycans by Distinct Receptors Unveiled by NMR and Molecular Modeling. *Front. Mol. Biosci.* **2021**, *8*, 727847.
(14) Gerken, T. A. The solution structure of mucous glycoproteins: proton NMR studies of native and modified ovine submaxillary mucin. *Arch. Biochem. Biophys.* **1986**, *247*, 239−253.
(15) Prendergast, J. M.; Galvao da Silva, A. P.; Eavarone, D. A.; et al. Novel anti-Sialyl-Tn monoclonal antibodies and antibody-drug conjugates demonstrate tumor specificity and anti-tumor activity. *MAbs* **2017**, *9*, 615−627.
(16) Loureiro, L. R.; Sousa, D. P.; Ferreira, D.; et al. Novel monoclonal antibody L2A5 specifically targeting sialyl-Tn and short glycans terminated by alpha-2−6 sialic acids. *Sci. Rep.* **2018**, *8*, No. 12196.
(17) Nuti, M.; Teramoto, Y. A.; Mariani-Costantini, R.; et al. A monoclonal antibody (B72.3) defines patterns of distribution of a novel tumor-associated antigen in human mammary carcinoma cell populations. *Int. J. cancer* **1982**, *29*, 539−545.
(18) Reddish, M. A.; Jackson, L.; Rao Koganty, R.; et al. Specificities of anti-sialyl-Tn and anti-Tn monoclonal antibodies generated using novel clustered synthetic glycopeptide epitopes. *Glycoconjugate J.* **1997**, *14*, 549−560.
(19) Ching, C. K.; Holmes, S. W.; Holmes, G. K. T.; Long, R. G. Comparison of two sialosyl-Tn binding monoclonal antibodies (MLS102 and B72.3) in detecting pancreatic cancer. *Gut* **1993**, *34*, 1722.
(20) Kurosaka, A.; Kitagawa, H.; Fukui, S.; et al. A monoclonal antibody that recognizes a cluster of a disaccharide, NeuAc alpha(2-

https://doi.org/10.1021/jacsau.4c00921
JACS Au 2025, 5, 225−236

6)GalNAc, in mucin-type glycoproteins. *J. Biol. Chem.* **1988**, *263*, 8724−8726.
(21) Ogata, S.; Koganty, R.; Reddish, M.; et al. Different modes of sialyl-Tn expression during malignant transformation of human colonic mucosa. *Glycoconjugate J.* **1998**, *15*, 29−35.
(22) Kjeldsen, T.; et al. Preparation and characterization of monoclonal antibodies directed to the tumor-associated O-linked sialosyl-2−−6 alpha-N-acetylgalactosaminyl (sialosyl-Tn) epitope. *Cancer Res.* **1988**, *48*, 2214−2220.
(23) Terasawa, K.; Furumoto, H.; Kamada, M.; Aono, T. Expression of Tn and sialyl-Tn antigens in the neoplastic transformation of uterine cervical epithelial cells. *Cancer Res.* **1996**, *56*, 2229−2232.
(24) Victorzon, M.; Nordling, S.; Nilsson, O.; Roberts, P. J.; Haglund, C. Sialyl Tn antigen is an independent predictor of outcome in patients with gastric cancer. *Int. J. Cancer* **1996**, *65*, 295−300.
(25) Foote, J.; Milstein, C. Conformational isomerism and the diversity of antibodies. *Proc. Natl. Acad. Sci. U.S.A.* **1994**, *91*, 10370−10374.
(26) Ma, B.; Zhao, J.; Nussinov, R. Conformational selection in amyloid-based immunotherapy: Survey of crystal structures of antibody-amyloid complexes. *Biochim. Biophys. Acta, Gen. Subj.* **2016**, *1860*, 2672−2681.
(27) Videira, P. A. Q.et al. L2A5 Antibody or Functional Fragment Thereof Against Tumour Antigens. WO2019/147152.2019.
(28) Li, C.; Palma, A. S.; Zhang, P.; et al. Noncovalent microarrays from synthetic amino-terminating glycans: Implications in expanding glycan microarray diversity and platform comparison. *Glycobiology* **2021**, *31*, 931−946.
(29) Marchetti, R.; Perez, S.; Arda, A.; et al. Rules of Engagement" of Protein-Glycoconjugate Interactions: A Molecular View Achievable by using NMR Spectroscopy and Molecular Modeling. *ChemistryOpen* **2016**, *5*, 274−296.
(30) Ereño-Orbea, J.; Sicard, T.; Cui, H.; et al. Structural Basis of Enhanced Crystallizability Induced by a Molecular Chaperone for Antibody Antigen-Binding Fragments. *J. Mol. Biol.* **2018**, *430*, 322−336.
(31) Lenza, M. P.; Egia-Mendikute, L.; Antoñana-Vildosola, A.; et al. Structural insights into Siglec-15 reveal glycosylation dependency for its interaction with T cells through integrin CD11b. *Nat. Commun.* **2023**, *14*, No. 3496.
(32) Kuroki, K.; Wang, J.; Ose, T.; et al. Structural basis for simultaneous recognition of an O-glycan and its attached peptide of mucin family by immune receptor PILRα. *Proc. Natl. Acad. Sci. U.S.A.* **2014**, *111*, 8877−8882.
(33) Kiessling, L. L.; Diehl, R. C. CH-π Interactions in Glycan Recognition. *ACS Chem. Biol.* **2021**, *16*, 1884−1893.
(34) Kufe, D. W. Mucins in cancer: function, prognosis and therapy. *Nat. Rev. Cancer* **2009**, *9*, 874−885.
(35) Bhatia, R.; Gautam, S. K.; Cannon, A.; et al. Cancer-associated mucins: role in immune modulation and metastasis. *Cancer Metastasis Rev.* **2019**, *38*, 223−236.
(36) Corzana, F.; Busto, J. H.; Jiménez-Osés, G.; et al. Serine versus threonine glycosylation: the methyl group causes a drastic alteration on the carbohydrate orientation and on the surrounding water shell. *J. Am. Chem. Soc.* **2007**, *129*, 9458−9467.
(37) Movahedin, M.; Brooks, T.; Supekar, N.; et al. Glycosylation of MUC1 influences the binding of a therapeutic antibody by altering the conformational equilibrium of the antigen. *Glycobiology* **2017**, *27*, 677−687.
(38) Amon, R.; Grant, O. C.; Leviatan Ben-Arye, S.; et al. A combined computational-experimental approach to define the structural origin of antibody recognition of sialyl-Tn, a tumor-associated carbohydrate antigen. *Sci. Rep.* **2018**, *8*, 10786.
(39) Blixt, O.; Hurtado-Guerrero, R.; Gatos, S. Combotope Antibody Libraries. US2024/0309110A1, 2024.

https://doi.org/10.1021/jacsau.4c00921
JACS Au 2025, 5, 225−236